Calbindin D_{28k} EF-Hand Ligand Binding and Oligomerization: Four High-Affinity Sites—Three Modes of Action†

Tommy Cedervall,‡,§ Ingemar André,§ Cheryl Selah,‡ James P. Robblee,|| Peter C. Krecioch,|| Robert Fairman,|| Sara Linse,*,‡ and Karin S. Åkerfeldt*,‡

Departments of Chemistry and Biology, Haverford College, Haverford, Pennsylvania 19041, and Department of Biophysical Chemistry, Lund University, Post Office Box 124, S221 00 Lund, Sweden

Received May 10, 2005; Revised Manuscript Received June 29, 2005

ABSTRACT: Calbindin D_{28k}, a highly conserved protein with Ca^{2+}-sensing and Ca^{2+}-buffering capabilities, is abundant in brain and sensory neurons. This protein contains six EF-hand subdomains, four of which bind Ca^{2+} with high affinity. Calbindin D_{28k} can be reconstituted from six synthetic peptides corresponding to the six EF-hands, indicating a single-domain structure with multiple interactions between the EF-hand subdomains. In this study, we have undertaken a detailed characterization of the Ca^{2+}-binding and oligomerization properties of each individual EF-hand peptide using CD spectroscopy and analytical ultracentrifugation. Under the conditions tested, EF2 is monomeric and does not bind Ca^{2+}, whereas EF6, which binds Ca^{2+} weakly, aggregates severely. We have therefore focused this study on the high-affinity binding sites, EF-hands 1, 3, 4, and 5. Our sedimentation equilibrium data show that, in the presence of Ca^{2+}, EF-hands 1, 3, 4, and 5 all form dimers in solution in which the distribution between the monomer, dimer, and higher order oligomers differs. The processes of Ca^{2+} binding and oligomerization are linked to different degrees, and three main mechanisms emerge. For EF-hands 1 and 5, the dimer binds Ca^{2+} more strongly than the monomer and Ca^{2+} binding drives dimerization. For EF-hand 4, dimer formation requires only one of the monomers to be Ca^{2+}-bound. In this case, the Ca^{2+} affinity is independent of dimerization. For EF-hand 3, dimerization occurs both in the absence and presence of Ca^{2+}, while oligomerization increases in the presence of Ca^{2+}.

The association behavior of single EF-hand subdomains may provide structural information on the corresponding native protein. It is expected that the oligomerization properties of isolated subdomains are more complex for buried compared to peripheral EF-hands. We have explored this concept for six synthetic EF-hand peptides derived from calbindin D_{28k} to elucidate their structural position within the protein. As expected, the peptide association is strongly coupled to Ca^{2+} binding, and this has been analyzed in detail.

The EF-hand is one of the most populated structural folds identified to date (*1*). The 29-residue sequence motif constitutes a characteristic helix−loop−helix structure that typically provides a medium to high-affinity Ca^{2+}-binding site. Figure 1 shows the amino acid variation in the 29 positions of the consensus sequence. When all residues that are found in at least 5% of the EF-hands are counted (*2*), 4×10^{18} different sequences can be constructed that adhere to the EF-hand consensus sequence. This enormous sequence variability allows for regulation of Ca^{2+} affinity, tuning of specific interactions between EF-hands, and binding of distinct cellular targets with high precision. The seemingly simple EF-hand is a versatile building block that can make up proteins with a remarkable variation in structure and function (*3*).

The smallest entity, a single EF-hand, has been found in prokaryotes (*4*, *5*). In eukaryotes, EF-hands are arranged in domains consisting of two or more subdomains. The pairing of EF-hands buries nonpolar residues and allows for the possibility of cooperative Ca^{2+} binding. The basic pairwise subdomain arrangement is found in a variety of proteins, including calmodulin and troponin C. EF-hand pairs are also found within larger domains. The sarcoplasmic Ca^{2+}-binding protein (*6*) and recoverin (*7*) are examples of proteins with four EF-hands in a single domain. The S100 proteins are homodimers of a polypeptide chain containing two EF-hands (*8*−*10*). Domains with an odd number of EF-hands are rare; however, in parvalbumin (*11*) and oncomodulin (*12*), extensive hydrophobic interactions lead to the assembly of three EF-hands (for a review, see ref *13*). The calpains are complex dimeric thiol proteases with five EF-hand subdomains in each chain.

† This work was supported by NSF Career Grant 9996074, the Lise Meitner Foundation, Lund University, Sweden, and the Henry Dreyfus Foundation (to K.S.Å.), the Swedish Research Council and the Wenner−Gren Foundation (to S.L.), and NSF Grant 9817188 (to R.F.).

* To whom correspondence should be addressed. Telephone: +1-610-896-1213. Fax: +1-610-896-4963. E-mail: kakerfel@haverford.edu (K.S.Å.); Telephone: +46-46-2228246. Fax: +46-46-2224543. E-mail: sara.linse@bpc.lu.se (S.L.).

‡ Department of Chemistry, Haverford College.

§ Lund University.

|| Department of Biology, Haverford College.

10.1021/bi050861q CCC: $30.25
Published on Web 09/21/2005

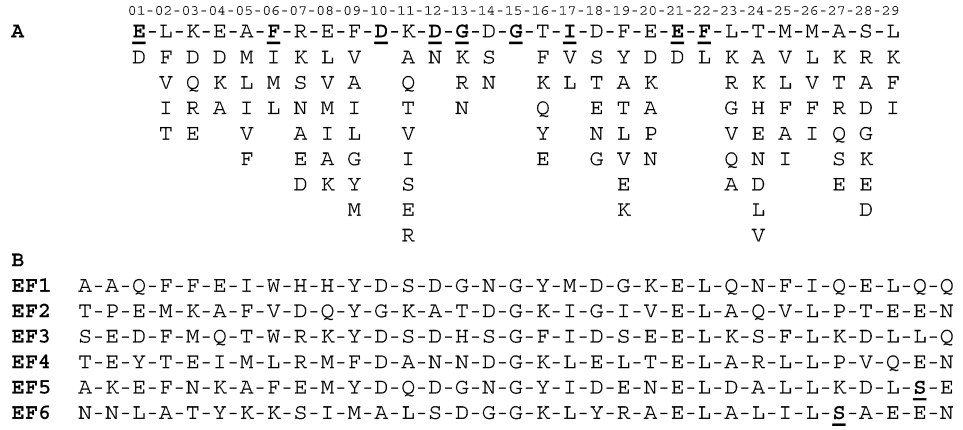

FIGURE 1: (A) Ca^{2+}-binding EF-hand motif, including residues found in at least 5% of the sequences in the database (*2*). Residues found in more than 50% of the sequences are highlighted in bold and underlined. (B) Amino acid sequences of synthesized peptides representing the six EF-hand subdomains in chicken calbindin D_{28k}. Cysteine residues are replaced by serine (in bold and underlined).

Studies of isolated EF-hands reveal a remarkable specificity in the interactions between EF-hand subdomains. Single EF-hand peptides derived from troponin C (*14*, *15*), calbindin D_{9k} (*16*), and parvalbumin (*17*, *18*) form homodimers in the presence of Ca^{2+}. When the peptides are mixed with their natural EF-hand partner, however, they strongly prefer to heterodimerize (*15*, *19*, *20*). Investigations on calmodulin reveal that steric complementarity of hydrophobic side chains at the subdomain interface and electrostatic repulsion in one of the homodimers provide a molecular basis for this specificity (*21*).

The high specificity in EF-hand recognition is apparent also with larger fragments. Tryptic digestion of the sarcoplasmic Ca^{2+}-binding protein effectively cuts the protein in two halves, each including one EF-hand pair. The halves form homodimers, but the heterodimer is strongly preferred (*22*). Similar results are obtained with fragments of parvalbumin (*23*, *24*) and calbindin D_{28k} (*25*, *26*). Thus, EF-hands that are removed from their natural partners tend to oligomerize to avoid unfavorable exposure of hydrophobic surfaces to the aqueous environment. In contrast, fragments that represent discrete globular domains of EF-hand proteins are not prone to oligomerization. This has been shown with sedimentation equilibrium (SE)[1] experiments for calretinin (*27*), gel filtration for calmodulin (E. Thulin, personal communication), and high-resolution structural studies for calmodulin (*28*, *29*) and troponin C (*30*, *31*).

Calbindin D_{28k} represents one of the larger EF-hand proteins with six EF-hands in a single domain (*32*, *26*) in which EF-hands 1, 3, 4, and 5 bind Ca^{2+} with high affinity (*33*−*35*). The single-domain structure of calbindin D_{28k} implies that there are extensive contacts beyond the pairwise arrangement, which raises the possibility that its isolated subdomains may bind Ca^{2+} and self-associate in a more complex manner than the EF-hands from smaller domains. For example, it was previously found that an EF-hand from S100B, which is part of a four EF-hand domain, forms tetramers (*36*).

The present work focuses on the assocation behavior of EF-hand subdomains originating from calbindin D_{28k} (Figure 1). In particular, we address the linkage between Ca^{2+} binding and self-assocation. The difference in oligomerization behavior may report on the position of the EF-hands relative to one another within the protein in which a more buried subdomain would be expected to display a more complex oligomerization pattern compared to a subdomain located closer to the protein surface. In this study, CD spectroscopy and analytical ultracentrifugation have been employed. The two methods provide very similar results showing that the individual EF-hands indeed behave in distinct manners. Three different modes of coupling between Ca^{2+} binding and oligomerization are observed, which illustrates the diversity and complexity of these correlated processes.

MATERIALS AND METHODS

Calbindin D_{28k} EF-Hand Peptides: Preparation and Nomenclature. Peptides, 33 amino acid residues long and representing EF-hands 1−6 of chicken calbindin D_{28k} (Figure 1) were synthesized and purified as previously described (*33*). The regions linking the EF-hand regions were omitted, and the cysteine residues were replaced by serine. EF1 and EF6 represent the N- and C-terminal EF-hand sequence, respectively.

Ca^{2+} Titration as Monitored by Circular Dichroism (CD) Spectroscopy. The peptide concentration of the stock solutions was determined by amino acid analysis (Keck Facility at Yale University, CT). The EF3, EF4, and EF5 peptides were dissolved in 2 mM Tris/HCl at pH 7.5. The buffer was Ca^{2+}-depleted prior to the titrations, as previously described (*37*). EF3, EF4, and EF5 were diluted to various concentrations in the same buffer, and each sample was titrated with Ca^{2+} by adding 2 μL aliquots of 5, 20, 100, or 200 mM $CaCl_2$. The CD signal was monitored at 222 nm at 25 °C using a 1 mm quartz cuvette and an Aviv 62DS CD spectropolarimeter. Various concentrations of EF1, in 2 mM Tris/HCl at pH 8.0, were titrated with 2 μL aliquots of $CaCl_2$. The CD signals at 212 and 222 nm were recorded on a Jasco J-720 spectropolarimeter at 25 °C using a 2 mm quartz cuvette.

Analysis of Ca^{2+} Binding for EF1, EF3, EF4, and EF5. The Ca^{2+}-binding data were analyzed using a five-state model in which the peptide can occupy the following states: apo monomer (A), Ca_1 monomer (ACa), apo dimer (A_2), Ca_1 dimer (A_2Ca), or Ca_2 dimer (A_2Ca_2). The Ca^{2+}-binding (K_1, K_1^d, K_2) and dimerization (K_a^{apo}, K_a, K_a^{Ca})

[1] Abbreviations: SE, sedimentation equilibrium; ssMW, single-species molecular weight; log, ^{10}log.

constants are defined as follows:

$$K_1 = \frac{[\mathrm{ACa}]}{[\mathrm{A}][\mathrm{Ca}]} \quad (1)$$

$$K_a = \frac{[\mathrm{A_2Ca}]}{[\mathrm{A}][\mathrm{ACa}]} \quad (2)$$

$$K_2 = \frac{[\mathrm{A_2Ca_2}]}{[\mathrm{A_2Ca}][\mathrm{Ca}]} \quad (3)$$

$$K_a^{\mathrm{Ca}} = \frac{[\mathrm{A_2Ca_2}]}{[\mathrm{ACa}]^2} \quad (4)$$

$$K_a^{\mathrm{apo}} = \frac{[\mathrm{A_2}]}{[\mathrm{A}]^2} \quad (5)$$

$$K_1^{\mathrm{d}} = \frac{[\mathrm{A_2Ca}]}{[\mathrm{A_2}][\mathrm{Ca}]} \quad (6)$$

Free energy is a state variable, and because two thermodynamic cycles can be constructed (Figure 2), only four of the six binding constants are necessary to describe the system. At any point in the Ca^{2+}-titration experiment the following equation holds:

$$\mathrm{Ca_{tot}} = [\mathrm{Ca}] + [\mathrm{ACa}] + [\mathrm{A_2Ca}] + 2[\mathrm{A_2Ca_2}] \quad (7)$$

A similar type of equation can be constructed for the peptide

$$\mathrm{A_{tot}} = [\mathrm{A}] + [\mathrm{ACa}] + 2[\mathrm{A_2Ca}] + 2[\mathrm{A_2Ca_2}] + 2[\mathrm{A_2}] \quad (8)$$

Ca_{tot} and A_{tot} are the total concentrations of Ca^{2+} and peptide, respectively. Substituting eqs 1−3 into eq 7 gives

$$[\mathrm{Ca}] + K_1[\mathrm{A}][\mathrm{Ca}] + K_1K_a[\mathrm{A}]^2[\mathrm{Ca}] + 2K_1K_aK_2[\mathrm{A}]^2[\mathrm{Ca}]^2 - \mathrm{Ca_{tot}} = 0 \quad (9)$$

Substitution of eqs 2−4 and 6 into eq 8 gives

$$\mathrm{A_{tot}} = [\mathrm{A}] + K_1[\mathrm{A}][\mathrm{Ca}] + 2K_1K_a[\mathrm{A}]^2[\mathrm{Ca}] + 2K_1K_aK_2[\mathrm{A}]^2[\mathrm{Ca}]^2 + 2K_a^{\mathrm{apo}}[\mathrm{A}]^2 \quad (10)$$

The contribution, Y_i, from each peptide species, i, to the CD signal is assumed to be proportional to the concentration of that species, and m_i is the proportionality constant.

$$Y_{\mathrm{A}} = m_{\mathrm{A}}[\mathrm{A}] \quad (11)$$

$$Y_{\mathrm{ACa}} = m_{\mathrm{ACa}}[\mathrm{ACa}] \quad (12)$$

$$Y_{\mathrm{A_2Ca}} = m_{\mathrm{A_2Ca}}[\mathrm{A_2Ca}] \quad (13)$$

$$Y_{\mathrm{A_2Ca_2}} = m_{\mathrm{A_2Ca_2}}[\mathrm{A_2Ca_2}] \quad (14)$$

$$Y_{\mathrm{A_2}} = m_{\mathrm{A_2}}[\mathrm{A_2}] \quad (15)$$

The spectroscopic signal is obtained by summation of the contributions of the different peptide species and addition of the background signal, b.

$$Y = Y_{\mathrm{A}} + Y_{\mathrm{ACa}} + Y_{\mathrm{A_2Ca}} + Y_{\mathrm{A_2Ca_2}} + Y_{\mathrm{A_2}} + b \quad (16)$$

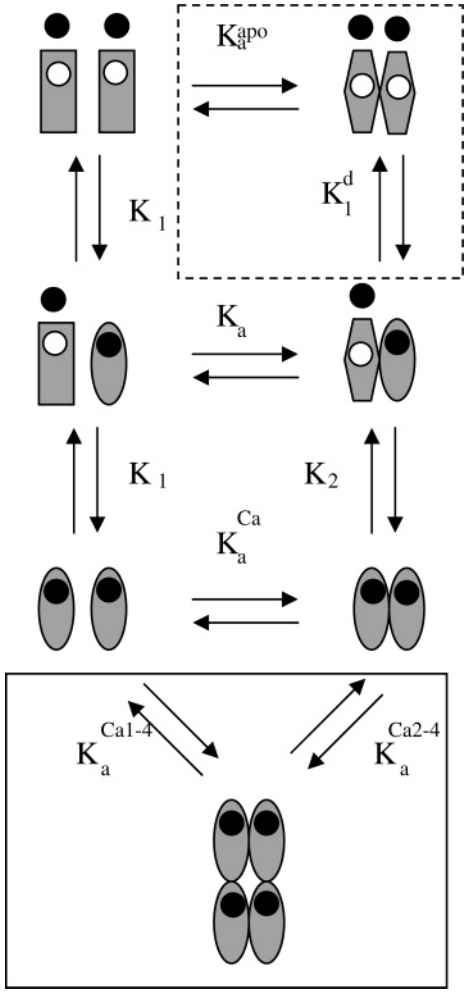

FIGURE 2: Five-state model, adapted from Julenius et al. (*16*), including dimerization of peptides and Ca^{2+} binding to monomers and dimers. The six-state model also includes a tetramer (boxed).

To solve for the free Ca^{2+} and apo monomer concentration, A, in each titration step, eqs 9 and 10 must be solved. Equation 9 can be solved analytically, whereas eq 10 is solved numerically by using the zbrent method (*38*). This method uses a combination of bisection, secant, and inverse quadratic interpolation methods.

The Ca^{2+}-binding parameters were fitted numerically by optimizing χ^2

$$\chi^2 = \sum_{i=1}^{N}\left[\frac{Y_i - Y(a)}{\sigma_i}\right]^2 \quad (17)$$

in which Y_i represents the experimentally obtained spectroscopic signal, $Y(a)$ represents the calculated value of Y using the parameter set a, and σ_i represents the standard deviation of point i. A Levenberg−Marquardt algorithm was used for the χ^2 optimization (*38*). This algorithm requires that partial derivatives be calculated for the different parameters, which were determined numerically. Preliminary binding parameters were obtained by fitting each peptide concentration to a 1:1

Table 1: Global Single-Species Analysis of Data from Sedimentation Equilibrium of Calbindin D_{28k} EF-Hand Peptides

EF-hand	MW (kDa), theoretical	[peptide] (μM)	MW (kDa), experimental			
			no salt	KCl[a]	$CaCl_2$[b]	$CaCl_2$/KCl
EF1	4.000	20		4.21 ± 0.49[c]	7.47 ± 0.34	7.38 ± 0.39
		100	4.00 ± 0.24	4.36 ± 0.18	9.54 ± 0.59	8.07 ± 0.33
EF2	3.633	100	2.94 ± 0.33	4.31 ± 0.33	4.17 ± 0.46	4.12 ± 0.44
EF3	4.036	20	2.43 ± 0.19	4.66 ± 0.39	10.28 ± 0.57	8.48 ± 0.59
		100	4.94 ± 0.29	9.63 ± 0.60	12.30 ± 0.48	12.08 ± 0.60
EF4	3.909	20	1.56 ± 0.11	4.01 ± 0.35	4.52 ± 0.58	6.52 ± 0.60
		100	1.86 ± 0.11	3.70 ± 0.37	8.71 ± 0.45	9.21 ± 0.46
		200	2.05 ± 0.11	4.06 ± 0.18	8.81 ± 0.55	9.93 ± 0.43
EF5	3.866	20		3.55 ± 0.35	7.22 ± 0.62	7.01 ± 0.42
		100	1.67 ± 0.13	4.97 ± 0.34	7.60 ± 0.30	6.75 ± 0.74
		200		4.74 ± 0.24	7.37 ± 0.26	7.01 ± 0.23
EF6	3.638	20−200		ND[d]	ND[d]	ND[d]

[a] The KCl concentration was 0.15 M. NaCl was also tested in some cases with similar results. [b] The $CaCl_2$ concentration was 10 mM. [c] Single-species molecular weight is obtained by simultaneously analyzing the data from sedimentation performed at 30, 40, and 50 krpm. [d] ND = not determined; EF6 aggregated at 30 krpm under all conditions.

peptide/Ca^{2+}-binding equilibrium

$$A + Ca \overset{K_1}{\rightleftharpoons} ACa \tag{18}$$

The values of K_1 for different peptide concentrations were interpreted and used as starting parameters for the expanded fit in which all of the different concentrations were included simultaneously. The errors in the fitted parameters were estimated from the square root of the covariance matrix. The *F* test was then used to calculate the significance of adding the extra parameters to the model

$$F = \frac{(N - n)(\chi_m^2 - \chi_n^2)}{(n - m)\chi_n^2} \tag{19}$$

where *N* is the number of data variables and *n* and *m* are the number of parameters in the compared models.

Ca^{2+}-Binding Analysis Including a Tetramer. In the analysis of the Ca^{2+}-binding data for EF1, EF3, and EF4, an extra sixth state was added to the original five-state model. In this model, monomers and dimers are assumed to form tetramers with binding constants K_a^{Ca1-4} and K_a^{Ca2-4}, respectively. Together with the dimerization equilibrium for Ca^{2+}-bound peptide, these two equilibria form a thermodynamic cycle, which means that it is sufficient to add only one extra independent binding constant to the fit. K_a^{Ca1-4} and K_a^{Ca2-4} are defined as

$$K_a^{Ca1-4} = \frac{[A_4Ca_4]}{[ACa]^4} \tag{20}$$

$$K_a^{Ca2-4} = \frac{[A_4Ca_4]}{[A_2Ca_2]^2} \tag{21}$$

Equation 9 is expanded with a higher order term, and the Ca^{2+} concentration is solved for using the Newton−Raphson method.

Analytical Ultracentrifugation. Stock solutions of each peptide were made in H_2O, and the concentrations were determined by a modified ninhydrin colorimetric analysis (*39*). Solutions were neutralized with KOH. Peptide solutions (20, 100, and 200 μM) were made in 2 mM Tris/HCl at pH 7.5 or with the addition of 0.15 M KCl, 10 mM $CaCl_2$, or both 10 mM $CaCl_2$ and 0.15 M KCl. SE experiments were carried out using a Beckman Optima XL-A analytical ultracentrifuge. The samples were loaded at several peptide concentrations into a six-channel charcoal-filled Epon centerpiece (12 mm path length), equipped with quartz windows. The samples were run at 25 °C at 30 000, 40 000 and 50 000 rpm using an AN-60 Ti rotor. After equilibration for 12 h, 20 scans were obtained and averaged. Analysis was done with the Nonlin algorithm (*40*) obtained from the Analytical Ultracentrifugation Facility at the University of Connecticut (Storrs, CT). The partial specific volume for each peptide was calculated as the weighted average of the partial specific density of each constituent amino acid, and ρ was calculated as the sum of the approximate change in density for each buffer component added to the density of water as described in Laue et al. (*41*). The data were fitted initially with a single species model. Depending on the complexity of the data, more complex, self-association models were considered as well (i.e., monomer−dimer and monomer−dimer−tetramer).

RESULTS

Oligomerization of Calbindin D_{28k} EF-Hand Peptides. The oligomerization state of individual EF-hand peptides was studied by SE. The EF-hands were analyzed at different peptide concentrations with or without 10 mM $CaCl_2$ and in buffer with or without KCl. In the absence of KCl and $CaCl_2$, the single-species molecular weight (ssMW) is close to or below the calculated monomer molecular weight for EF1, EF2, EF4, and EF5, indicating that no oligomerization occurs (Table 1). An ssMW below the theoretical MW is likely due to charge density effects because there are large net negative charges ($Z = -3$ to -6) for the apo peptides. In 0.15 M KCl, the charge is sufficiently shielded to yield ssMW values around the calculated monomer MW (Table 1). One of the apo peptides, EF3, clearly oligomerizes in the absence as well as in the presence of KCl. In 0.1 M KCl, ssMW increases from 4.7 to 9.6 kDa when the peptide concentration is increased from 20 to 100 μM. In 10 mM $CaCl_2$, with or without 0.15 M KCl, all peptides, except EF2, display a MW higher than expected for the monomer, indicative of self-association. The ssMW values for EF1, EF4, and EF5 are about twice the expected molecular weight, suggesting that the peptides dimerize. EF3 displays a ssMW that is 3 times

Table 2: Estimated Molecular Weight (in Kilodaltons) from Single-Species Analysis of Sedimentation Equilibrium Analytical Ultracentrifugation Data for EF3[a]

conditions	rotor speed (rpm)		
	30 000	40 000	50 000
no salt	5.8	5.1	4.8
0.15 M KCl	11.3	10.1	8.8
10 mM $CaCl_2$	13.1	12.4	11.6
KCl and $CaCl_2$	13.5	12.4	11.1

[a] Peptide (100 μM) in 2 mM Tris/HCl at pH 7.5.

the expected molecular weight, implying higher order oligomerization. When the results are taken together, they show that EF1, EF3, EF4, and EF5 form dimers or multimers in the presence of Ca^{2+}, while EF2 is monomeric under all experimental conditions tested. EF6 could not be studied because of severe aggregation. This peptide has a large fraction of hydrophobic residues and zero net charge.

In the presence of $CaCl_2$, the ssMW values increase with increasing peptide concentration for EF1, EF3, and EF4. Furthermore, analysis of the ssMW at each rotor speed used in the experiment shows that the ssMW values decrease with increasing rotor speed (as exemplified in Table 2). When the results are taken together, they indicate that EF1, EF3, and EF4 are in equilibrium between two or more species rather than existing as a single species. To determine the oligomerization state of the complexes, the data were fitted with different models (Table 3). The square root of variance, a measure of goodness of fit, is used to determine the best-fit models. In the absence of Ca^{2+}, EF1 and EF4 are close to the expected monomeric molecular weight. Because the molecular weight is slightly higher than expected, they may both exist in a monomer−dimer (1−2) equilibrium, strongly favoring the monomer. In the presence of Ca^{2+}, the best fit comes from a monomer−dimer−tetramer (1−2−4) equilibrium. The best model for EF3 is also a 1−2−4 equilibrium, both with and without $CaCl_2$. The addition of $CaCl_2$ favors dimers and tetramers; however, it must be noted that it is difficult, if not impossible, to distinguish between a 1−2−4 model and a 1−2−3 model. These models were compared in the calculation of self-assocation constants. Given the lack of peptide concentration dependence for the ssMW, as determined by SE, EF5 is largely monomeric in the absence of $CaCl_2$ and largely dimeric in the presence of $CaCl_2$, making it difficult to accurately determine the peptide association constant.

Ca^{2+} Titration of EF1, EF3, EF4, and EF5. Peptides EF1, EF3, EF4, EF5, and EF6 were all previously shown to display a concentration-dependent helical structure, as determined by CD spectroscopy (*33*). The addition of Ca^{2+} also increases the helical content, indicating that the peptides bind Ca^{2+} and undergo a conformational change. In contrast, EF2 displays little helical structure both in the presence and absence of Ca^{2+}. To determine the affinity between the single EF-hand peptides and Ca^{2+}, EF1, EF3, EF4, and EF5 were titrated with Ca^{2+} at several peptide concentrations at low salt (2 mM Tris/HCl at pH 7.5) and the conformational change was followed by recording the CD signal at 222 nm. EF6 was excluded from the study because of its tendency to self-associate and precipitate (*33*). All peptides show a saturable increase of the CD signal (parts A−D of Figure 3) upon addition of an increasing amount of Ca^{2+}. To estimate the individual Ca^{2+}-binding constants, the data for each peptide concentration were first fitted by a simplified 1:1 binding model, in which one Ca^{2+} ion interacts with one EF-hand peptide and the CD signal differs between the bound and free forms. This situation corresponds to the left portion of the equilibrium outlined in Figure 2, involving only K_1. For EF3 and EF4, this approach yielded apparent Ca^{2+}-association constants that were independent of the peptide concentration. Log K_1 was determined to be 4.6 for EF3 and 3.3 for EF4. In contrast, the apparent K_1 for EF1 and EF5 increases with an increasing peptide concentration, indicating that Ca^{2+} binding to these peptides is influenced by oligomerization. To further investigate the link between Ca^{2+} binding and oligomerization, the titration data were analyzed using a more complete model (Figure 2). The same approach was previously used in the analysis of Ca^{2+} binding to the two EF-hand peptides derived from calbindin D_{9k} (*16*). The data were thus fitted using a five-state model, including Ca^{2+} binding to both monomeric and dimeric EF-hand peptides (Figure 2). EF3 and EF4 were also reanalyzed in this way because the SE data clearly show a Ca^{2+}-driven oligomerization for these peptides. The results of the more complete analysis of each individual peptide are described below.

EF1. EF1 was titrated with Ca^{2+} at a peptide concentration ranging from 10 to 100 μM. Because the SE experiments suggest that the apo form of EF1 is monomeric, K_a^{apo} was omitted in the initial analysis, yielding a four-state model (Figure 2). The best fit is shown in Figure 3A, yielding the following association and dimerization constants: log K_1 = 3.4; log K_2 = 4.7; log K_a = 3.4; and log K_a^{Ca} = 4.7 (Table 4). Because the linked equilibria form a thermodynamic cycle (Figure 2), only three constants, log K_1, log K_2, and log K_a, are needed in the fitting procedure and log K_a^{Ca} was derived from their values. Adding K_a^{apo} to allow for the five-state model does not improve the fit (not shown). The values of the binding constants imply that dimeric EF1 binds Ca^{2+} stronger than the monomer. The peptide association constant, log K_a^{Ca} = 4.7, agrees with that obtained from fitting the SE data, log K_a^{Ca} = 5.2. The fact that the two different methods independently produce very similar results for the same parameter, log K_a^{Ca}, further validates the analyses. Both methods are also in agreement with the absence of an apo dimer. In conclusion, dimerization of EF1 is Ca^{2+}-dependent, and peptide dimerization enhances the Ca^{2+} affinity. Mutual enhancement is expected for processes forming a thermodynamic cycle.

The Ca^{2+}-binding data for EF1 were also analyzed with an expanded model, including a tetramer (see Figure 2), but no improvement to the fits was achieved (data not shown), presumably because these peptides do not form a substantial amount of tetramer, which is consistent with the SE experiments.

EF3. As described above, the apparent K_1 from the simplified analysis is independent of the peptide concentration. Simultaneous fitting of Ca^{2+} titrations at different peptide concentrations using a single binding constant yields an apparent log K_1 of 4.5. The data were analyzed using the five-state model resulting in a significantly lower χ^2. The SE experiments suggest that EF3 exists in a monomer−dimer equilibrium in the absence of Ca^{2+}, and therefore, K_a^{apo} was

Table 3. Analytical Ultracentrifugation Data Were Fitted Using Different Models[a]

peptide, conditions[b]		model								
		SS[c]	mon[d]	dim[e]	1−2	1−3	1−4	1−2−3	1−2−4	1−3−6
EF1	apo, KCl	3.74	4.26	20.39	3.76	3.81	3.85			
	$CaCl_2$	6.91	23.25	7.38	15.5		4.63	NF[f]	4.16	4.63
	$CaCl_2$, KCl	4.36	21.50	4.37	4.17	6.28	10.07	3.46	3.41	6.29
EF3	apo, KCl	6.05	14.05	6.25	6.24	2.97	2.64	3.21	2.47	2.48
	$CaCl_2$	4.36		10.08		3.26	5.29	3.26	2.86	2.86
	$CaCl_2$, KCl	6.12	19.19	8.65		4.02	4.19	4.47	3.21	3.23
EF4	apo, KCl	3.16	3.17		3.14	3.13	3.13	3.14		
	$CaCl_2$	7.32	15.91	7.34	7.09	4.50	4.90	4.75	4.51	4.46
	$CaCl_2$, KCl	5.54	20.59	7.64	6.60	3.26	5.68	3.10	3.05	3.27
EF5	apo, KCl	2.69	3.84	9.65	2.54	2.59	2.69	2.54	2.54	
	$CaCl_2$	2.65	14.14	2.87	2.61	4.37	2.61	2.61	2.61	4.37
	$CaCl_2$, KCl	4.60	12.49	5.43	4.68	6.80	8.07	4.68	4.68	6.81

[a] The results are reported as square roots of variance. [b] 10 mM $CaCl_2$ and 0.15 M KCl. [c] Single species. [d] Monomer. [e] Dimer. [f] NF = no fit.

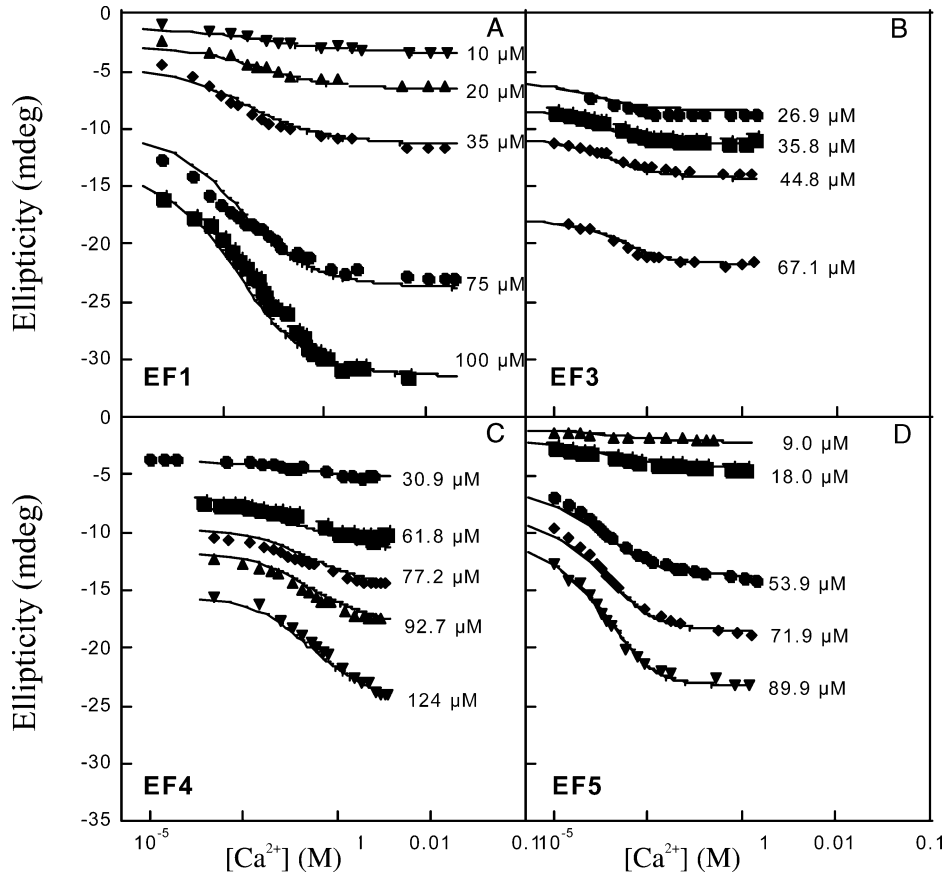

FIGURE 3: Ca^{2+} titrations for EF1, EF3, EF4, and EF5 with the CD signal monitored at 222 nm. The solid lines show the best simultaneous fit to the data at all peptide concentrations using the five-state model (EF3) or a four-state model omitting the apo dimer (EF1, EF4, and EF5). (A) EF1. (B) EF3. (C) EF4. (D) EF5.

included in the analysis. The small change seen in ellipticity after the addition of Ca^{2+} (see Figure 3B), in combination with the low peptide concentrations and the low value of K_a^{apo}, made the fitting rather insensitive to this parameter. log K_a^{apo} was therefore fixed to 2.9, the value obtained from SE analyses. The other binding constants were determined with higher precision as follows: log $K_1 = 3.2$; log $K_2 = 5.6$; log $K_a^{Ca} = 7.1$. Attempts to fit the data using the expanded model including a tetramer did not lead to any significant reduction in χ^2. In summary, we conclude that EF3 dimerizes both with and without Ca^{2+} and that dimerization and oligomerization increases in the presence of Ca^{2+}. The Ca^{2+} affinity is 300 times higher for the EF3 dimer than for the monomer.

EF4. The initial analyses of the data from Ca^{2+} titration of the EF4 peptide at different concentrations indicate that Ca^{2+} binding is independent of dimerization. Simultaneous fitting of Ca^{2+} titrations at different peptide concentrations using a single binding constant yields an apparent log K_1 of 2.3. A significantly better fit is achieved using the four-state model (Figure 3C) omitting K_a^{apo}. log K_1 and log K_2 are 3.6 and 3.4, respectively, confirming that EF4 binds Ca^{2+} independently from the peptide dimerization process. Furthermore, log K_a and log K_a^{Ca} are estimated to similar values, 4.4 and 4.1, respectively, which agrees with a log K_a^{Ca} of 3.8 as determined from the SE analysis (Table 4). Fitting to the data using the model including a tetramer does not improve the fit (not shown).

Table 4: Ca^{2+}-Binding (log K_1 and log K_2) and Peptide-Association (log K_a^{apo} and log K_a^{Ca}) Constants[a]

	sedimentation equilibrium			Ca^{2+} titrations			
	low salt		0.15 M KCl	low salt			
EF-hand	log K_a^{apo}	log K_a^{Ca}	log K_a^{Ca}	log K_a	log K_a^{Ca}	log K_1	log K_2
EF1		5.2	5.4	3.4	4.7	3.4	4.7
EF3	2.9	8.8 ± 1.6	5.0	4.7	7.1 ± 0.3	3.2	5.6 ± 0.3
EF4		3.8	5.0	4.4	4.1	3.6	3.4
EF5		5.5	5.0	2.5	4.5	4.5	6.5

[a] The errors in the log K values are within ± 0.2 or less unless otherwise indicated.

EF5. The EF5 Ca^{2+} titration data at different peptide concentrations yielded log K_1 values ranging from 4.7 to 5.6 using a two-state model, indicating that Ca^{2+} binding is influenced by the dimerization of the peptide. When the data are fitted using the four-state model (Figure 3D) omitting the apo dimer, the obtained binding constants are log $K_1 =$ 4.5, log $K_2 = 6.5$, log $K_a = 2.5$, and log $K_a^{Ca} = 4.5$. Hence, the Ca^{2+} affinity for the dimer is much higher than for the monomer. The value of log K_a^{Ca} is lower than that obtained from SE (log $K_a^{Ca} = 5.7$, Table 4). As noted above, Ca^{2+}-loaded EF5 is predominantly dimeric, making it difficult to accurately estimate an association constant from the SE data. Including K_a^{apo} in the model or using a model in which a tetramer is included does not improve the fit. EF5 follows a mechanism similar to EF1, but the Ca^{2+} affinity is significantly higher for EF5.

DISCUSSION

In many biological systems, ligand binding is coupled to the association of protein components. Such situations require a combination of methods and complex data analysis to extract a complete picture of the equilibrium states. Here, we have successfully combined SE and ligand-binding assays at different peptide concentrations to determine Ca^{2+}-binding affinities, oligomerization states, and self-association constants of individual EF-hands. The information from the SE experiments is used to limit the number of parameters in the fit using the complex model describing the Ca^{2+}-binding process. From these analyses, we can draw the following conclusions about the behavior of the subdomains from calbindin D_{28k}.

All six EF-hands from calbindin D_{28k} display unique behavior from which three major mechanisms may be distilled. In mechanism 1 (Figure 4), Ca^{2+} binding enhances dimerization and the Ca^{2+} affinity is higher for the dimer than the monomer. This is observed for EF1 and EF5. In the case of EF5, two Ca^{2+}-bound EF-hands associate 100-fold more strongly than two apo peptides and the Ca^{2+} affinity is 100-fold higher for the dimer than for the monomer. EF5 does not form oligomers beyond the dimer. This is in agreement with the well-resolved ^{1}H NMR spectra obtained at the same peptide concentrations in which the line widths are typical of a two EF-hand entity (*33*). For EF1, dimerization requires only one peptide to be bound to Ca^{2+}, but the association is stronger between two Ca^{2+}-loaded monomers. Ca^{2+}-loaded EF1 also has a tendency to form larger complexes than dimers.

In mechanism 2 (Figure 4), which is observed for EF4, the Ca^{2+} affinity is the same for the monomer and dimer and the association constant for dimerization is the same regardless of whether one or two peptides are Ca^{2+}-loaded.

A distinct mechanism, mechanism 3 (Figure 4), is seen for EF3, which dimerizes both with and without Ca^{2+} (although oligomerization increases in the presence of Ca^{2+}). The Ca^{2+} affinity is considerably higher for the dimer than for the monomer. The apo dimer and Ca^{2+}-driven oligomerization are supported by previous results (*33*) in which CD spectroscopy is consistent with EF3 being helical in the absence of Ca^{2+}. Only small changes are seen after addition of Ca^{2+}, indicating that the helical structure is largely unaffected. The observed broad signals in the one-dimensional ^{1}H NMR spectra (*33*) may also indicate oligomerization of Ca^{2+}-free EF3 or exchange processes that occur on an intermediate time scale. After the addition of Ca^{2+}, the signals are broadened further, which may be due to the formation of yet larger structures. A structural change involving mostly the tertiary structure is not expected to display a change in the CD spectra. Therefore, a model in which the dimerization is Ca^{2+}-independent whereas tetramerization or higher oligomerization is Ca^{2+}-dependent can explain these results for EF3.

EF2 and EF6 cannot be placed in any of the three mechanisms because both lack high-affinity Ca^{2+}-binding sites. EF2 does not bind Ca^{2+} at all nor does it dimerize under any of the experimental conditions used in this study. Previous studies show that EF6 binds Ca^{2+} weakly and undergoes a conformational change after Ca^{2+} binding (*33*), but in the SE experiments, this peptide displays a strong tendency for aggregation, preventing further analysis in this study.

A domain consisting of two or more EF-hands allows for cooperative Ca^{2+} binding. The coupling of Ca^{2+}-binding events is manifested in different ways, with negative (*42*), positive (*16*, *17*), or no (*16*) cooperativity in Ca^{2+} binding. Positive cooperativity is in effect when the Ca^{2+} affinity of one site is enhanced by Ca^{2+} binding to another site. If the sites are covalently linked, as in a native protein, cooperativity is straightforward to evaluate. In a nonlinked system, however, as in the present case, cooperativity may be defined in more than one way. One definition involves the ratio of K_2/K_1^d, the two Ca^{2+}-binding constants in the dimer (Figure 2). Another possibility is to compare K_2 with K_1, i.e., the second Ca^{2+}-binding event in the dimer with the Ca^{2+} affinity for the monomer. For most EF-hands in this study, the apo dimer cannot be invoked and K_1^d cannot be determined. We therefore use the ratio of K_2/K_1 as a measure of cooperativity. For statistical reasons, there is positive cooperativity when $K_2/K_1 > 0.25$. For EF1, EF3, and EF5, the ratio K_2/K_1 is very large (20, 400, and 100, respectively) and there is strong

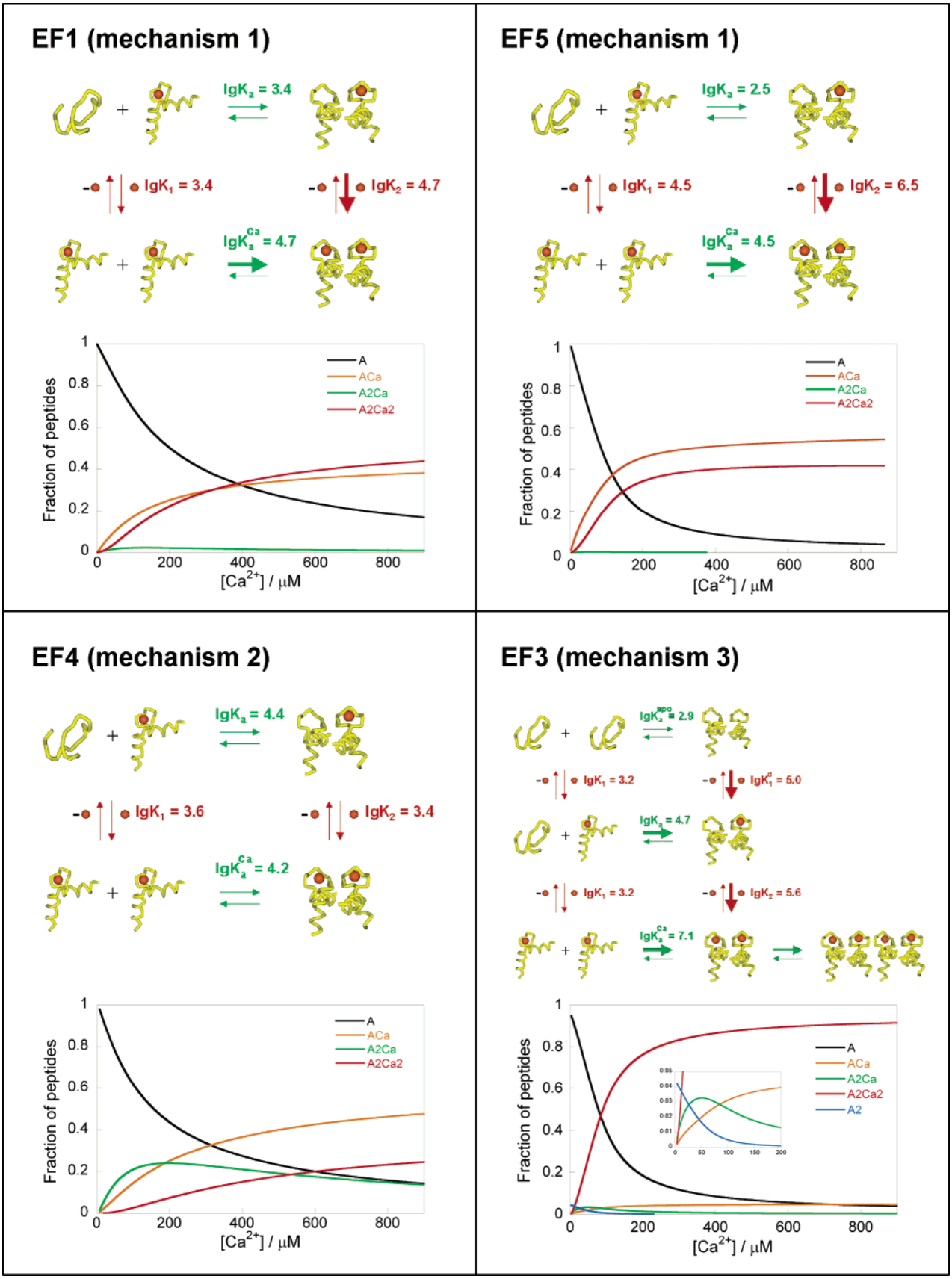

FIGURE 4: Three major mechanisms for the coupled processes of Ca^{2+} binding and peptide association. The top half of each panel shows a scheme, simplified from Figure 2, including the parameters as obtained from fitting the Ca^{2+}-titration data. Ca^{2+}-binding constants are shown in red, and peptide-association constants are shown in green. The bottom half of each panel shows the fraction of peptides engaged in different species, A, A_2, ACa, A_2Ca, and A_2Ca_2, as a function of the total Ca^{2+} concentration as calculated for 100 μM of EF1, EF3, EF4, or EF5. The inset for EF3 is a *y* expansion of the region between 0 and 200 μM Ca^{2+}.

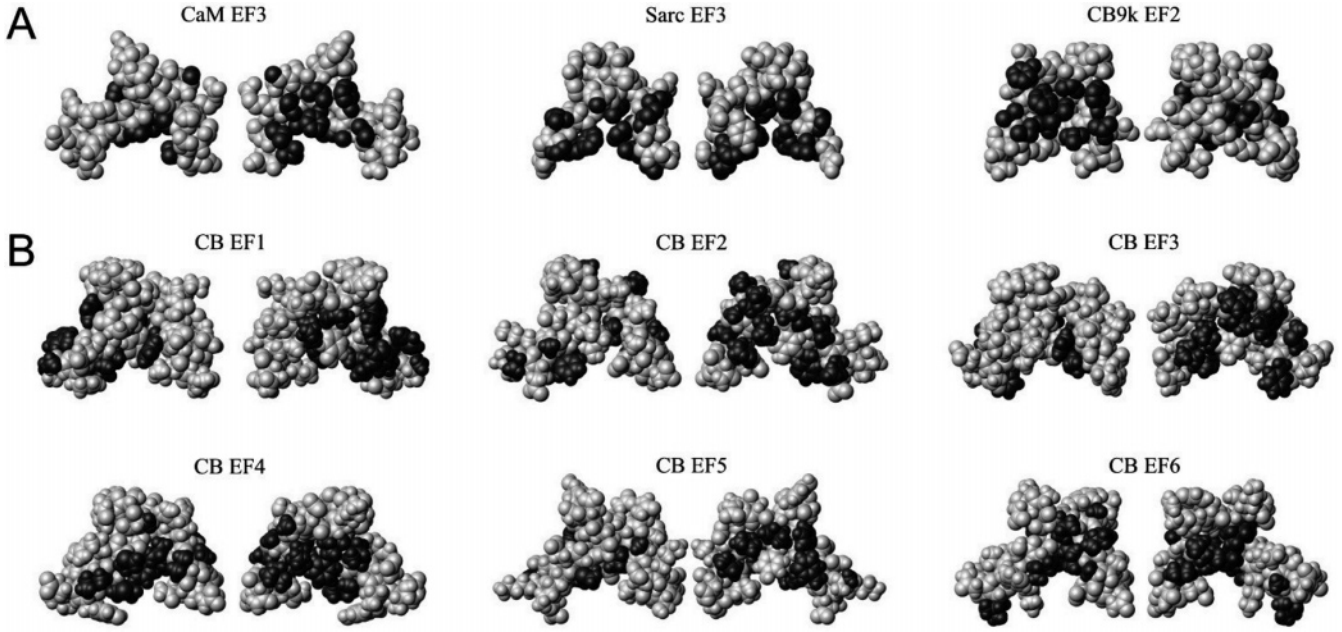

FIGURE 5: (A) EF3 from calmodulin (PDB code 1CLL), EF3 from sarcoplasmic Ca^{2+}-binding protein (PDB code 2SCP), and EF2 from calbindin D_{9k} (PDB code 4ICB) shown as space-filling models with the hydrophobic side chains in dark gray and the backbone and hydrophilic side chains in light gray. Both sides of each EF-hand is displayed. (B) Models of the calbindin D_{28k} EF-hands 1−6 built on the calmodulin EF3 backbone (PDB code 1CLL) with the same shading scheme as above. The backbone was fixed, and the calbindin D_{28k} side chains were optimized using Swiss PDB Modeller (*44*).

positive cooperativity of Ca^{2+} binding. In contrast, for EF4, K_2/K_1 is around 0.6, implying a low degree of cooperativity. It is interesting to compare the distribution of different species during the coupled events of Ca^{2+} binding and peptide association for the four high-affinity EF-hands (Figure 4). In the case of EF3, the high degree of positive cooperativity manifests itself as a strongly coupled process. The two main species present during the Ca^{2+} titration are the apo monomer and Ca^{2+}-saturated dimer, with only small amounts of all possible intermediates (Figure 4). In contrast, for EF1, EF4, and EF5, intermediates are present to different extents.

For most of the calbindin D_{28k} subdomains, dimerization is strongly coupled to Ca^{2+} binding. The SE experiments in low salt indicate that a high density of negative charges, as in EF4 and EF5, leads to extensive repulsion between peptides, which is observed as an apparent molecular weight below the calculated monomeric weight. In 150 mM KCl, the molecular weight agrees with that for the monomer, showing that the salt effectively screens the negative charges but does not induce dimerization. Instead, the formation of dimers and higher order oligomers of EF1, EF4, and EF5 is a Ca^{2+}-specific process. In contrast, dimerization of EF3 can be induced by the addition of 150 mM KCl and is further strengthened by Ca^{2+} binding.

The distribution of polar and nonpolar residues is strikingly distinct in EF-hands derived from globular domains containing different numbers of subdomains. For example, the C-terminal domain of calmodulin consists of two subdmains, EF3 and EF4. The interface between EF3 and EF4 is predominantly hydrophobic, while the outside surface facing the solvent is predominantly polar (for EF3, see the left of Figure 5A). A similar situation is observed for the two EF-hands present in the small globular protein calbindin D_{9k} (for EF2, see the right of Figure 5A). In the sarcoplasmic Ca^{2+}-binding protein, the interactions between the four subdomains are more extensive and the distribution of polar and nonpolar side chains is more complex (for EF3, see the middle of Figure 5A).

High-resolution structural data are, so far, unavailable for calbindin D_{28k}; however, the structural positions of the subdomains may be inferred from the results of the present study. Molecular modeling was used to predict the distribution of polar and nonpolar residues within each subdomain. Three models of each subdomain were built on the backbone coordinates of calmodulin EF3 (PDB code 1CLL), calbindin D_{9k} EF2 (PDB code 4ICB), and the sarcoplasmic Ca^{2+}-binding protein EF3 (PDB code 2SCP). In all three cases, the modeling gives a similar distribution of polar and nonpolar groups (Figure 5B). The modeling suggests that the six EF-hands from calbindin D_{28k} are most similar to those in the sarcoplasmic Ca^{2+}-binding protein. The EF-hand subdomains in calbindin D_{28k} all display a relatively complex hydrophobic surface pattern, in particular, EF4 and EF6. The propensity to form interactions beyond the pairwise EF-hand arrangement is manifested in the complex dimerization and oligomerization properties of the isolated EF-hands. The higher order oligomers observed by SE for EF3 and EF4 suggest that, in intact calbindin D_{28k}, these EF-hands are in contact with more than one other subdomain. This is consistent with the molecular modeling in which particularly EF4 displays multiple hydrophobic patches, again implying contacts with more than one subdomain. The model of EF6 shows the most complex pattern of hydrophobic patches, implying a buried position. This is consistent with its tendency to aggregate, and its folding has also been found to depend on the presence of other subdomains (*32*). The dimeric nature of EF5 may reflect interactions with fewer partners within the intact protein. Although EF2 does not bind Ca^{2+} nor folds on its own, its structure is induced in the presence of other subdomains (*32*). The addition of EF1 is not sufficient to induce folding of EF2 (*32*), but when

covalently linked, the EF1−EF2 fragment is folded (*25*), suggesting that it forms a pair within the intact protein. The EF1−EF2 and EF1−EF2−EF3 fragments form homodimers in solution (*25*, *26*), suggesting that EF1 and/or EF2 form additional contacts within the intact protein. In summary, our results suggest that EF6 is the most buried subdomain. EF2, EF3, and especially EF4 appear to engage in multiple contacts within the protein, while EF1 and, in particular, EF5 are likely to be closer to the surface with only one face contacting the rest of the protein.

In native calbindin D_{28k}, the four high-affinity sites have similar affinities for Ca^{2+} (*35*). When excised from the protein, the Ca^{2+} affinity is in each case reduced by approximately 3 orders of magnitude (Table 4). This implies that interactions within the intact protein are important for maintaining high Ca^{2+} affinity. The small variation (within a factor of 10) among the isolated EF-hands points to different degrees of affinity modulation by the protein scaffold. In particular, EF1 and EF4 appear to depend to a large extent on interactions with other EF-hands (Table 4 and Figure 4).

Previous findings show that calbindin D_{28k} contains one domain including all six EF-hands (*32*). In this study, we have shown that there is a strong tendency for the calbindin D_{28k} EF-hand peptides to form larger aggregates than dimers, in analogy with the observed tetramer formation of an EF-hand derived from the sarcoplasmic Ca^{2+}-binding protein, which also consists of a larger domain (*36*). The association behavior of single EF-hands can thus yield information that directly pertains to their function *in vivo*. It is likely that all six EF-hands of calbindin D_{28k} cooperate in the structural and functional response of this protein, which has been shown to be involved in cellular signaling (*43*).

This study describes an approach for delineating the Ca^{2+} binding and oligomerization properties of single EF-hands. Furthermore, the linkage between these two processes has been investigated. Three main mechanisms have emerged from this work that form a basis for understanding the properties of the native protein calbindin D_{28k}. The method should be applicable to other systems in which ligand binding is coupled to oligomerization.

REFERENCES

1. Day, R., Beck, D. A. C., Armen, R. S., and Daggett, V. (2003) A consensus view of fold space: Combining SCOP, CATH, and the Dali Domain Dictionary, *Protein Sci. 12*, 2150−2160.
2. Falke, J. J., Drake, S. K., Hazard, A. L., and Peersen, O. B. (1994) Molecular tuning of ion binding to calcium signaling proteins, *Q. Rev. Biophys. 27*, 219−290.
3. Nelson, M. R., and Chazin, W. J. (1998) Structures of EF-hand Ca^{2+}-binding proteins: Diversity in the organization, packing, and response to Ca^{2+} binding, *Biometals 11*, 297−318.
4. Vyas, M. N., Jacobson, B. L., and Quiocho, F. A. (1987) A novel calcium binding site in the galactose-binding protein of bacterial transport and chemotaxis, *Nature 327*, 635−638.
5. van Asselt, E. J., and Dijkstra, B. W. (1999) Binding of calcium in the EF-hand of *Escherichia coli* lytic transglycosylase Slt35 is important for stability, *FEBS Lett. 458*, 429−435.
6. Vijay-Kumar, S., and Cook, W. J. (1992) Structure of sarcoplasmic calcium-binding protein from *Nereis diversicolor* refined at 2.0 Å resolution, *J. Mol. Biol. 224*, 413−426.
7. Flaherty, K. M., Zozulya, S., Stryer, L., and McKay, D. B. (1993) Three-dimensional structure of recoverin, a Ca^{2+} sensor in vision, *Cell 75*, 709−716.
8. Potts, B. C., Smith, J., Akke, M., Macke, T. J., Okazaki, K., Hidaka, H., Case, D. A., and Chazin, W. J. (1995) The structure of calcyclin reveals a novel homodimeric fold for S100 Ca^{2+}-binding proteins, *Nat. Struct. Biol. 2*, 790−796.
9. Drohat, A. C., Amburgey, J. C., Abildgaard, F., Starich, M. R., Baldisseri, D., and Weber, D. J. (1996) Solution structure of rat apo-S100B($\beta\beta$) as determined by NMR spectroscopy, *Biochemistry 35*, 11577−11588.
10. Drohat, A. C., Baldisseri, D. M., Rustandi, R. R., and Weber, D. J. (1998) Solution structure of Ca^{2+}-bound rat S100B($\beta\beta$) as determined by nuclear magnetic resonance spectroscopy, *Biochemistry 37*, 2729−2740.
11. Kretsinger, R. H., and Nockolds, C. E. (1973) Carp muscle Ca^{2+}-binding protein. II. Structure determination and general description, *J. Biol. Chem. 248*, 3313−3326.
12. Ahmed, F. R., Przybylska, M., Rose, D. R., Birnbaum, G. I., Pippy, M. E., and MacManus, J. P. (1990) Structure of oncomodulin refined at 1.85 Å resolution. An example of extensive molecular aggregation via Ca^{2+}, *J. Mol. Biol. 216*, 127−140.
13. Lewit-Bentley, A., and Réty, S. (2000) EF-hand calcium-binding proteins, *Curr. Opin. Struct. Biol. 10*, 637−643.
14. Shaw, G. S., Hodges, R. S., and Sykes, B. D. (1990) Calcium-induced peptide association to form an intact protein domain: ^{1}H NMR structural evidence, *Science 249*, 280−283.
15. Shaw, G. S., Hodges, R. S., and Sykes, B. D. (1992) Determination of the solution structure of a synthetic two-site calcium-binding homodimeric protein domain by NMR spectroscopy, *Biochemistry 31*, 9572−9580.
16. Julenius, K., Robblee, J., Thulin, E., Finn, B. E., Fairman, R., and Linse, S. (2002) Coupling of ligand binding and dimerization of helix−loop−helix peptides: Spectroscopic and sedimentation analyses of calbindin D_{9k} EF-hands, *Proteins 47*, 323−333.
17. Franchini, P. L. A., and Reid, R. E. (1999a) A model for circular dichroism monitored dimerization and calcium binding in an EF-hand synthetic peptide, *J. Theor. Biol. 199*, 199−211.
18. Franchini, P. L. A., and Reid, R. E. (1999) Investigating site-specific effects of the -X glutamate in a parvalbumin CD site model peptide, *Arch. Biochem. Biophys. 372*, 80−88.
19. Finn, B. E., Kordel, J., Thulin, E., Sellers, P., and Forsén, S. (1992) Dissection of calbindin D_{9k} into two Ca^{2+}-binding subdomains by combination of mutagenesis and chemical cleavage, *FEBS Lett. 298*, 211−214.
20. Berggård, T., Julenius, K., Ogard, A., Drakenberg, T., and Linse, S. (2001) Fragment complementation studies of protein stabilization by hydrophobic core residues, *Biochemistry 40*, 1257−1264.
21. Linse, S., Voorhies, M., Norström, E., and Schultz, D. A. (2000) An EF-hand phage display study of calmodulin subdomain pairing, *J. Mol. Biol. 296*, 473−486.
22. Durussel, I., Luan-Rilliet, Y., Petrova, T., Takagi, T., and Coz, J. A. (1993) Cation binding and conformation of tryptic fragments of Nereis sarcoplasmic calcium-binding protein: Calcium-induced homo- and heterodimerization, *Biochemistry 32*, 2394−2400.
23. Permyakov, E. A., Medvedkin, V. N., Mitin, Y. V., and Kretsinger, R. H. (1991) Noncovalent complex between domain AB and domains CD*EF of parvalbumin, *Biochim. Biophys. Acta 1076*, 67−70.
24. Henzl, M. T., Agah, S., and Larsson, J. D. (2003) Characterization of the metal ion-binding domains from rat α- and β-parvalbumins, *Biochemistry 42*, 3594−3607.
25. Klaus, W., Grzesiek, S., Labhardt, A. M., Buchwald, P., Hunziker, W., Gross, M. D., and Kallick, D. A. (1999) NMR investigation and secondary structure of domains I and II of rat brain calbindin D_{28k} (1−93), *Eur. J. Chem. 262*, 933−938.
26. Berggård, T., Thulin, E., Åkerfeldt, K. S., and Linse, S. (2000) Fragment complementation of calbindin D_{28k}, *Protein Sci. 9*, 2094−2108.
27. Palczewska, M., Groves, P., Ambrus, A., Kaleta, A., Kövér, K. E., Batta, G., and Kuźnicki, J. (2001) Structural and biochemical characterization of neuronal calretinin domain I−II (residues 1−100). Comparison to homologous calbindin D_{28k} domain I−II (residues 1−93), *Eur. J. Biochem. 268*, 6229−6237.
28. Finn, B. E., Drakenberg, T., and Forsén, S. (1993) The structure of apo-calmodulin. A ^{1}H NMR examination of the carboxy-terminal domain, *FEBS Lett. 336*, 368−374.
29. Ishida, H., Takahashi, K., Nackashima, K.-I., Kumaki, Y., Nakata, M., Hikichi, K., and Yazawa, M. (2000) Solution structures of the N-terminal domain of yeast calmodulin: Ca^{2+}-dependent conformational change and its functional implication, *Biochemistry 39*, 13660−13668.

30. Findlay, W. A., Sönnichsen, F. D., and Sykes, B. D. (1994) Solution structure of the TR_1C fragment of skeletal muscle troponin-C, *J. Biol. Chem. 269*, 6773.
31. Strynadka, N. C., Cherney, M., Sielecki, A. R., Li, M. X., Smillie, L. B., and James, M. N. (1997) Structural details of a calcium-induced molecular switch: X-ray crystallographic analysis of the calcium-saturated N-terminal domain of troponin C at 1.75 Å resolution, *J. Mol. Biol. 273*, 238−255.
32. Linse, S., Thulin, E., Gifford, L. K., Radzewsky, D., Hagan, J., Wilk, R. R., and Åkerfeldt, K. S. (1997) Domain organization of calbindin D_{28k} as determined from the association of six synthetic EF-hand fragments, *Protein Sci. 6*, 2385−2396.
33. Åkerfeldt, K. S., Coyne, A. N., Wilk, R. R., Thulin, E., and Linse, S. (1996) The Ca^{2+}-binding stoichiometry of calbindin D_{28k} as assessed by spectroscopic analyses of synthetic peptide fragments, *Biochemistry 35*, 3662−3669.
34. Veenstra, T. D., Johnson, K. L., Tomlinson, A. J., Naylor, S., and Kumar, R. (1997) Determination of calcium-binding sites in rat brain calbindin by electrospray ionization mass spectrometry, *Biochemistry 36*, 3535−3542.
35. Berggård, T., Miron, S., Onnerfjord, P., Thulin, E., Akerfeldt, K. S., Enghild, J. J., Akke, M., and Linse, S. (2002) Calbindin D_{28k} exhibits properties characteristic of a Ca^{2+} sensor, *J. Biol. Chem. 277*, 16662−16672.
36. Donaldson, C., Barber, K. R., Kay, C. M., and Shaw, G. S. (1995) Human S100b protein: Formation of a tetramer from synthetic calcium-binding site peptides, *Protein Sci. 4*, 765−772.
37. Linse, S. (2002) Calcium binding to proteins studied via competition with chromophoric chelators, *Methods Mol. Biol. 173*, 15−24.
38. Press, W. H., Teukolsky, S. A., Vetterling, W. T., and Flannery, B. P. (1992) *Numerical Recipes in C. The Art of Scientific Computing*, 2nd ed., Cambridge University Press, New York.
39. Rosén, H. (1957) A modified ninhydrin colorimetric analysis for amino acids, *Arch. Biochem. Biophys. 67*, 10−15.
40. Johnson, M. L., Correia, J. J., Yphantis, D. A., and Halvorson, H. R. (1981) Analysis of data from the analytical ultracentrifuge by nonlinear least squares techniques, *Biophys. J. 36*, 575−588.
41. Laue, T. M., Shah, B. D., Ridgeway, T. M., and Pelletier, S. L. (1992) Computer-aided interpretation of analytical sedimentation data for proteins, in *Analytical Ultracentrifugation in Biochemistry and Polymer Science* (Harding, S.E., Rowe, A.J., Horton, J.C., Eds.) pp 90−125, The Royal Society of Chemistry, Cambridge, U.K.
42. Shaw, G. S., Golden, l. F., Hodges, R. S., and Sykes, B. D. (1991) Interactions between paired calcium-binding sites in proteins: NMR determination of the stoichiometry of calcium binding to a synthetic troponin-C peptide, *J Am. Chem. Soc. 113*, 5557−5563.
43. Berggård, T., Szczepankiewicz, O., Thulin, E., and Linse, S. (2002) *myo*-Inositol monophosphatase is an activated target of calbindin D_{28k}, *J. Biol. Chem. 44*, 41954−41959.
44. Guex, N., and Peitsch, M. C. (1997) Swiss-modell and the Swiss-PDB Viewer: An environment for comparative protein modeling, *Electrophoresis 18*, 2714−2723.

BI050861Q